

Critical interfaces of the Ashkin-Teller model at the parafermionic point.

M. Picco¹ and R. Santachiara²

¹ *LPTHE³, Université Pierre et Marie Curie-Paris6*

Boîte 126, Tour 24-25, 5 ème étage,

4 place Jussieu, F-75252 Paris CEDEX 05, France,

e-mail: picco@lpthe.jussieu.fr.

² *LPTMS⁴, Université Paris-Sud*

Bâtiment 100

F-91405 Orsay, France,

e-mail: raoul.santachiara@lptms.u-psud.fr.

(Dated: May 5, 2010)

ABSTRACT

We present an extensive study of interfaces defined in the Z_4 spin lattice representation of the Ashkin-Teller (AT) model. In particular, we numerically compute the fractal dimensions of boundary and bulk interfaces at the Fateev-Zamolodchikov point. This point is a special point on the self-dual critical line of the AT model and it is described in the continuum limit by the Z_4 parafermionic theory. Extending on previous analytical and numerical studies [10, 12], we point out the existence of three different values of fractal dimensions which characterize different kind of interfaces. We argue that this result may be related to the classification of primary operators of the parafermionic algebra. The scenario emerging from the studies presented here is expected to unveil general aspects of geometrical objects of critical AT model, and thus of $c = 1$ critical theories in general.

³Unité mixte de recherche du CNRS UMR 7589.

⁴Unité mixte de recherche du CNRS UMR 8626

1 Introduction and motivation

The study of the scaling limit of interfaces in systems at criticality has been shown to be a very fruitful field of investigation which provided deep insights in the comprehension of critical phenomena [1]. The richness of conformal symmetry in two dimension (2D) make the two-dimensional critical systems an ideal framework to study these issues. In particular, there is a variety of 2D critical models for which exact methods of conformal field theory (CFT), combined with an available Coulomb-gas representation [2], allow the exact computation of all geometrical exponents characterizing the fractal shape of critical interfaces [3]. Among these models, we mention for instance the critical percolation, the self-avoiding walks, the loop erased random walks, or again spin lattice models such as the Potts models [1]. These studies have benefited from a great amount of numerical work [4] supporting the proposed theoretical scenario. In general, the critical models whose geometrical properties are well understood, even if there are often no rigorous proofs, can be associated to the critical phases of a one-parameter family of statistical models, the $O(n)$ loop models, the parameter n representing the loop fugacity. A remarkable recent development came with the introduction of the Schramm-Loewner evolution (SLE) which constitutes a family of conformally invariant stochastic growth process characterized by a parameter κ [5]. The SLE approach offers a conceptually new description of certain boundary interfaces defined in the $O(n)$ models.

The critical points of 2D systems can be classified according to different CFT families. Each family is characterized by a given set of (infinite) symmetries and the associated chiral current algebra. The representation theory of these algebras is at the basis of CFT constructions. The critical phases of the $O(n)$ models are described by the most simple of such CFT family, i.e. the one associated to the conformal symmetry alone and thus to the corresponding Virasoro algebra [6]. The connection between this family of CFTs and SLE approach has been fully understood [7]. However, there are other families of CFTs, the so called extended CFTs, which, besides the conformal symmetry, enjoy additional infinite symmetries. These theories describe universality classes which are different from the ones of the $O(n)$ models. A variety of statistical lattice models described by extended CFT have been introduced and studied since long time. Typically, these models are characterized by symmetries of some internal degrees of freedom, such as for instance the $SU(2)$ spin rotational symmetry in the quantum 1 + 1 spin chains [8]. The role of the additional symmetries, in particular for the so called rational CFT (RCFT), is well understood for many aspects, as, for instance, the operator algebra of the primary operators, or the classification of the conformal boundary conditions. Nevertheless, despite all the recent activity and progress, the geometrical properties of critical interfaces defined in such extended CFT are in general not understood. Moreover, an SLE approach to describe extended CFT is not known. For this respect, the Z_N spin models offer an ideal laboratory to study these issues. These are lattice model of spins which take N values and interact via a nearest-neighbor potential which is invariant under a Z_N cyclic permutation of the N spin states. The Z_N spin models admit critical points, the so called Fateev-Zamolochikov (FZ) points, described by the parafermionic CFT which are extended RCFTs with Z_N symmetry [9]. The cases with $N = 2$ and $N = 3$ correspond respectively to the Ising and the three-states Potts model, which in turn are related to the critical phases of the $O(\sqrt{2})$ and $O(\sqrt{3})$ loop models. This is also manifest in the fact that the associated \mathcal{Z}_2 and \mathcal{Z}_3 parafermionic theories coincide with the $c = 1/2$ and $c = 4/5$ Virasoro minimal model M_3 and M_5 [6]. The role of the Z_N symmetry becomes instead crucial for $N \geq 4$ where the Virasoro algebra is not rich enough to describe the corresponding parafermionic theory.

In the Z_N spin lattice models, the boundary and bulk interfaces can be naturally defined and the role of the Z_N internal degree of freedom is quite explicit in their definition. Moreover the Z_N spin models are simple models to be studied numerically. For $N \geq 4$, a description of the spin interfaces in terms of a low-energy effective field theory is not known, as it is the case for the interfaces defined in the $O(n)$ models. For this reason, the geometric description of the Z_N spin models are for many aspects unknown. The study of the Z_N spin models at the FZ point is thus expected to provide general deep insights on the geometrical description of extended CFTs.

Numerical measurements of the fractal dimensions associated to the spin interfaces for Z_4 and Z_5 spin models at the FZ point were presented in [10, 11]. In [10] we considered these Z_4 and Z_5 spin models on a bounded domain and we investigated the properties of a boundary interface related to certain boundary conditions. The numerical results were in the agreement with the theoretical predictions in [12] where the fractal dimension of this interface on the basis of the hypothesis of an SLE with an additional stochastic

motion in the internal group of symmetry. This approach has been inspired by previous work on the connection between SLE and CFT with superconformal symmetries [13] or with additional Lie-group symmetries, [13, 14].

In order to further investigate the geometrical properties of Z_N spin models and the possible consistency with some proposed theoretical scenario, we studied systematically in [11] the bulk geometrical properties of spin and random cluster interfaces for the Z_4 and Z_5 models. These results clearly marked a difference in the behavior of these non local objects compared to the Ising or the three-states Potts model. Among these results there was the observation that the fractal dimension of certain spin bulk interfaces were different from the ones corresponding for the boundary interfaces in [10].

The Z_4 spin model is particularly interesting as it coincides with the Ashkin-Teller (AT) model. In [15] the fractal dimension of a boundary interface was investigated along the critical line of the AT. At the FZ point of the Z_4 spin model, the value of the fractal dimension was found consistent with the value of the interface studied in [12] and [10].

In this paper we consider in great detail the spin cluster interfaces of the Z_4 spin model at the FZ point by studying systematically different bulk and boundary interfaces. In order to interpret the numerical results, in particular in the light of their universal character, we discuss the classification of the Z_4 conformal boundary conditions in terms of boundary spin configurations.

The main result of this paper is the computation of three different values of fractal dimensions which may encode universal geometrical properties of the Z_4 FZ point. Even if this results lacks of a clear theoretical explanation, we point out, on the basis of the properties of the Z_4 CFT, a possible scenario for the geometrical properties of this extended CFT. It is important to stress that the Z_4 CFT coincides with a free Gaussian field compactified on an orbifold. The study of the AT interfaces complement thus the results known for the free Gaussian field compactified on a circle [16, 17, 18] and may suggest an emergent general behavior for critical interfaces in $c = 1$ critical theories.

2 The model

We first define the Z_4 spin model. On each site of a square lattice there is a spin which can take 4 values, $S_i = 1, \dots, 4$. The Hamiltonian defining the model under consideration can be written as

$$H_{Z_4} = - \sum_{\langle ij \rangle} A \delta_{S_i, S_j} + B \delta_{S_i, S_j \pm 1} + C \delta_{S_i, S_j \pm 2}, \quad (1)$$

where A, B, C are real nonnegative coefficients, $\delta_{S_i, S_j} = 1$ if $S_i = S_j \pmod{4}$ and 0 otherwise. Besides a constant irrelevant term, the interaction is described by two independent real parameters. The cyclic Z_4 symmetry of the model (1) is completely manifest. One has to remark that the above Hamiltonian is invariant under a bigger symmetry than Z_4 , namely the dihedral group D_4 symmetry acting on the spin degree of freedom. The Boltzmann weight corresponding to (1) reads:

$$\exp(-H_{Z_4}) = \prod_{\langle ij \rangle} \left[x_0 + 2x_1 \cos \frac{\pi(S_i - S_j)}{2} + x_2 \cos \pi(S_i - S_j) \right], \quad (2)$$

where, by setting the normalization $x_0 = 1$:

$$x_1 = \frac{\exp(A) - \exp(C)}{4} \quad x_2 = \frac{\exp(A) - 2\exp(B) + \exp(C)}{2}. \quad (3)$$

The Z_4 spin model can be considered as a generalisation of fourth-states Potts model, obtained by choosing $x_1 = x_2$ ($B = C$). The generalization to $x_1 \neq x_2$ consists in the possibility of having a non trivial weight between two non equal spins S_i and S_j which depends on the difference between these spins, *i.e.* $|S_i - S_j|$.

The Z_4 spin model (1) is a representation of the AT model [19]. An equivalent (and more standard) representation of the AT model is in terms of two coupled Ising models. In this Ising representation, on each site i of a square lattice one associates a pair of spins, denoted by σ_i and τ_i , which takes two values, say up(+) and down(-). The Hamiltonian is defined by

$$H_{AT} = - \sum_{\langle ij \rangle} K(\sigma_i \sigma_j + \tau_i \tau_j) + K_4 \sigma_i \sigma_j \tau_i \tau_j. \quad (4)$$

In this representation the two parameters, K and K_4 , correspond respectively to the usual Ising spin interaction and to the 4-spins coupling between two Ising models. One can pass from the representation (1) to the (4) via the correspondence:

$$\begin{aligned} S_i = 1 &\rightarrow \sigma_i = +, \tau_i = + ; \quad S_i = 2 \rightarrow \sigma_i = +, \tau_i = - \\ S_i = 3 &\rightarrow \sigma_i = -, \tau_i = - ; \quad S_i = 4 \rightarrow \sigma_i = -, \tau_i = + ; \end{aligned}$$

from which one can derive the following relation between $(K, K_4) \rightarrow (x_1, x_2)$:

$$\exp(4K) = \frac{1 + 2x_1 + x_2}{1 - 2x_1 + x_2} ; \quad \exp(2K + 2K_4) = \frac{1 + 2x_1 + x_2}{1 - x_2} . \quad (5)$$

The AT model on the square lattice is equivalent to the staggered six vertex model. It presents a rich phase diagram which has been very well studied [20, 21] : in particular the phase diagram shows a critical line which is defined, in the Ising representation, by the self-dual condition $\sinh 2K = \exp(-2K_4)$ and terminates at $\coth 2K_2 = 2$. By imposing the self-dual condition, the AT model can be solved by mapping it to the so called F model, a special case of a solvable six vertex model [21].

On the critical line one can identify three particular points : i) the fourth-states Potts model $K = K_4$ corresponding to $x_1 = x_2 = 1/3$, ii) the case of two decoupled critical Ising models, corresponding to $\sqrt{x_2} = x_1 = -1 + \sqrt{2}$ (where $K_4 = 0$) and iii) the so called Fateev Zamolodchikov (FZ) point defined by

$$x_1^{\text{FZ}} = \frac{\sin(\frac{\pi}{16})}{\sin(\frac{3\pi}{16})} ; \quad x_2^{\text{FZ}} = x_1 \frac{\sin(\frac{5\pi}{16})}{\sin(\frac{7\pi}{16})} . \quad (6)$$

The FZ point has been shown to be completely integrable [9]. The continuum limit of the AT model on the critical line is described by a free Gaussian field with action $\mathcal{S} = \frac{1}{4\pi} \int dz d\bar{z} \partial\phi \bar{\partial}\phi$ where the scalar field ϕ is compactified on a orbifold of radius r^{orb} , i.e. $\phi = \phi + 2\pi r^{\text{orb}}$ and $\bar{\phi} = -\phi$. The critical Potts, (Ising)² and FZ point corresponds respectively to $r^{\text{orb}} = 2, \sqrt{2}$ and $r^{\text{orb}} = \sqrt{3}$.

The Gaussian theory with $r^{\text{orb}} = \sqrt{3}$ describes the FZ point and coincides with the Z_4 parafermionic field theory [22]. In this paper we will mainly focus on the geometric critical properties of the FZ point.

3 Classification of \mathcal{Z}_4 boundary states and their spin representations

In this section we discuss the problem of the classification of the boundary states for the \mathcal{Z}_4 parafermionic theory. In particular we are interested in the representations of such states in terms of spin configurations. The reason is that we want to study interfaces which are generated by imposing special boundary spin configurations. A classification of conformal boundary states in terms of spin configuration can then be used to identify interfaces whose measure is conformally invariant.

The relation between certain spin configurations on the boundary and the conformal boundary states is known in the case of the Ising and three-states Potts model [23, 24, 25]. This is in general not true for the \mathcal{Z}_4 theory (and general \mathcal{Z}_N theory, $N \geq 4$), where only the spin representations of a small subset of boundary states has been explicitly discussed [26]. On the other hand, we mention that a complete characterization of parafermionic boundary states in terms of A-D-E lattice models degree of freedom has been accomplished in [27].

3.1 Rational CFTs: classification of conformal boundary conditions.

In the following we briefly review the algebraic formulation of boundary states for RCFTs [23, 28]. A RCFT is characterized by a certain chiral algebra and the corresponding Hilbert space contains a finite number of the chiral algebra irrep. $|j\rangle$ which closes under operator product expansion.

One of the main results of the boundary RCFT [29, 23] is the bijection between boundary conformal states, which we indicate as $|\bar{j}\rangle$, and the irrep. $|j\rangle$. In particular, the states $|\bar{i}\rangle$ can be expressed as:

$$|\bar{i}\rangle = \sum_j \frac{\mathcal{S}_{ij}}{\sqrt{\mathcal{S}_{0j}}} |j\rangle \quad (7)$$

where the matrix \mathcal{S}_{ij} determines the modular transformation properties of the partition function defined on a cylinder. For a RCFT the \mathcal{S} matrix is in general known. The notation $|0\rangle$ usually indicates the (trivial) identity representation.

We define $\mathcal{Z}_{\bar{i},\bar{j}}$ the partition function on a cylinder with boundary conditions $|\bar{i}\rangle$ and $|\bar{j}\rangle$ at the two ends. One has:

$$\mathcal{Z}_{\bar{i},\bar{j}} = \sum_i n_{i,\bar{j}}^i \chi_i(q) \quad (8)$$

where q is the modular parameter, the $n_{i,\bar{j}}^i$ is the number of copies of the representation $|i\rangle$ occurring in the spectrum and $\chi_i(q)$ is the character of the representation $|i\rangle$. A general boundary condition changing operator (b.c.c.) $\psi_{\bar{0},\bar{j}}$ produces a transition from the vacuum $|\bar{0}\rangle$ (related to the identity representation) and \bar{j} boundary condition. The b.c.c. $\psi_{\bar{0},\bar{j}}$ transforms in the representation j . In this case the cylinder partition function reduces to a single character as $n_{\bar{0},\bar{j}}^j = 1$ and

$$\mathcal{Z}_{\bar{0},\bar{j}} = \chi_j(q). \quad (9)$$

The formulas (8-9) are extremely useful: given a certain lattice model, one can compute numerically the corresponding partitions (8-9) for different boundary conditions on the cylinder. Then, by comparing these results with the boundary CFT data, one can in principle associate the CFT boundary states to specific configurations of the degrees of freedom defining the lattice model.

We specify the above equations for the \mathcal{Z}_N theories. Reminiscent of the coset construction of the parafermionic theories, $\mathcal{Z}_N = SU(2)_N/U(1)$, we use the notation (see [30]) $|l, m\rangle$, with $l = 0, 1/2, 1, \dots$ and m an integer to label the primaries of the \mathcal{Z}_N theory. In particular the set of distinct principal representations of the \mathcal{Z}_N theory is given by pairs $|l, m\rangle$ where $l = 0, 1/2, 1, \dots, N/2$, $m = -2l, -2l+2, \dots, 2N-2l-2$ with $2l+m = 0 \pmod{2}$. The representations $|l, m\rangle$ and $|N/2-l, k+m\rangle$ have to be identified. The corresponding boundary states $|\bar{l}, \bar{m}\rangle$ are defined by:

$$|\bar{l}', \bar{m}'\rangle = \sum_{l,m} \frac{\mathcal{S}_{l,m}^{l',m'}}{\mathcal{S}_{l,m}^{0,0}} |l, m\rangle \quad (10)$$

where $\mathcal{S}_{l,m}^{l',m'}$ is the modular transformation matrix [30]:

$$\mathcal{S}_{l,m}^{l',m'} = \frac{2}{\sqrt{N(N+2)}} e^{i\pi m m'/N} \sin \frac{\pi(2l+1)(2l'+1)}{N+2}. \quad (11)$$

3.2 A known example: Three-states Potts model

Before considering the Z_4 spin model, we would like to review the results in [23, 24, 25] concerning the critical Z_3 spin model, i.e. the critical three-states Potts model. In this case one can identify (almost) all the boundary states in terms of spin configurations with quite simply arguments. Still, the Z_3 model is enough rich to show some general properties of the Z_N spin models which we will try to generalize to the case $N = 4$.

The table of principal fields of the \mathcal{Z}_3 theory with the corresponding conformal dimension Δ is presented in Tab. 1. The fields $\Psi^{\pm 1}$ are the symmetry currents generating the Z_3 chiral algebra. It is useful to stress that the fields listed in the above table are primaries of the Virasoro algebra but not of the parafermionic one. Indeed one can group the \mathcal{Z}_3 Virasoro primary fields into two families, $\{I, \Psi^1, \Psi^{-1}\}$ and $\{\Phi^1, \varepsilon, \Phi^{-1}\}$ which in turn correspond to the two representation modules of Z_3 algebra. The fields in each module are thus connected one to the other by symmetry transformations, or, in other words, by acting with the modes of the $\Psi^{\pm 1}$ fields. This means that, taking into account (11), the boundary states in (10) transform under a Z_3 rotation as:

$$\begin{aligned} |\bar{0}, \bar{0}\rangle &\rightarrow |\bar{0}, \bar{2}\rangle \rightarrow |\bar{0}, \bar{4}\rangle \rightarrow |\bar{0}, \bar{0}\rangle \\ |\bar{1/2}, \bar{3}\rangle &\rightarrow |\bar{1/2}, \bar{1}\rangle \rightarrow |\bar{1/2}, \bar{-1}\rangle \rightarrow |\bar{1/2}, \bar{3}\rangle. \end{aligned} \quad (12)$$

Field	Δ	$ l, m \rangle$
I	0	$ 0, 0 \rangle$
Ψ^1	2/3	$ 0, 2 \rangle$
Ψ^{-1}	2/3	$ 0, 4 \rangle$
Φ^1	1/15	$ 1/2, 1 \rangle$
ε	2/5	$ 1/2, 3 \rangle$
Φ^{-1}	1/15	$ 1/2, -1 \rangle$

Table 1: Principal fields for the \mathcal{Z}_3 theory.

This two distinct Z_3 “orbifolds” can thus be directly related to the two already mentioned representation modules of the \mathcal{Z}_3 parafermionic algebra.

Conformal boundary states in the spin representation

In the three-states Potts model, where the spins can take the values 1, 2 or 3, the following boundary conditions have been considered [23, 24]:

- *free*: the spins can take the values 1, 2 or 3 with equal probability
- *fixed*: the spins take the value 1 or 2 or 3. There are thus three fixed boundary conditions.
- *mixed*: the spins can take with equal probability the value 1 or 2 (1 + 2), 2 or 3 (2 + 3), 1 or 2 (1 + 2). Again there are three mixed boundary conditions.

The transformation (12) greatly constraints the possible boundary states identifications. Indeed, once one identify the boundary state $|\overline{0}, \overline{0} \rangle$ with the fixed boundary condition (say when the spin are fixed to the value 1), the states $|\overline{0}, \overline{2} \rangle$ and $|\overline{0}, \overline{4} \rangle$ have to be associated to the other two fixed boundary conditions. Then, by observing that the free boundary conditions are invariant under a Z_3 rotation, one is led to associate the states $|1/2, 1 \rangle$, $|1/2, 3 \rangle$ and $|1/2, -1 \rangle$ to the other mixed boundary conditions. Finally, taking into account that $\mathcal{Z}_{(1|1+2)} = \mathcal{Z}_{(1|1+3)}$ (for the Z_3 symmetry), one can write:

$$\begin{aligned} \mathcal{Z}_{(1|1)} &= \chi_I, \quad \mathcal{Z}_{(1|2)} = \chi_{\Psi^1}, \quad \mathcal{Z}_{(1|3)} = \chi_{\Psi^{-1}} \\ \mathcal{Z}_{(1|1+2)} &= \chi_{\Phi^1} = \chi_{\Phi^{-1}} = \mathcal{Z}_{(1|1+3)}, \quad \mathcal{Z}_{(1|2+3)} = \chi_{\varepsilon}. \end{aligned} \quad (13)$$

To make the connection with the minimal model M_5 [6] with central charge 4/5 one has to take into account relations of the kind $\chi_I = \chi_{(1,1)} + \chi_{(4,1)}$ or $\chi_{\varepsilon} = \chi_{(1,2)} + \chi_{(1,3)}$ where $\chi_{(r,s)}$ is the Virasoro character of the operator $\phi_{(r,s)}$ in the minimal Kac table. The boundary operator ψ_{ε} transforming in the representation ε generates then the boundary conditions (1|2 + 3) and thus the interface $SLE_{24/5}$ discussed in [31].

One last remark: the six bulk operators which we have considered so far do not complete the set of primaries of the \mathcal{Z}_3 parafermionic theory. In general, the space of representation of a \mathcal{Z}_N theory includes also fields which are associated to the non-Abelian elements of the dihedral D_N group [32]. For the \mathcal{Z}_3 theory, the two principal fields in this sector, which we indicate as R_0 and R_1 , have respectively dimensions 1/8 and 1/40. The free boundary conditions have been associated with the representation R_0 [32]

$$\mathcal{Z}_{(1|free)} = \chi_{R_0}, \quad (14)$$

while the representation R_1 has been associated to a *new* boundary condition:

$$\mathcal{Z}_{(1|new)} = \chi_{R_1}. \quad (15)$$

The physical interpretation of the new b.c. in terms of spin variables is actually unclear [25].

Field	Δ	$ l, m\rangle$
I	0	$ 0, 0\rangle$
Ψ^1	3/4	$ 0, 2\rangle$
Ψ^{-1}	3/4	$ 0, 4\rangle$
Ψ^2	1	$ 0, 6\rangle$
$\Phi^{1/2}$	1/16	$ 1/2, -1\rangle$
ε'	9/16	$ 1/2, 3\rangle$
$\Phi^{-1/2}$	1/16	$ 1/2, 1\rangle$
ε''	9/16	$ 1/2, 5\rangle$
Φ^1	1/12	$ 1, 2\rangle$
ε	1/3	$ 1, 0\rangle$

Table 2: Principal fields for the \mathcal{Z}_4 theory.

The conformally invariant boundary states for the three-states Potts model are exhausted [33] by the eight boundary states (13), (14) and (15). Finally, one can check these identifications by verifying that the partition function associated to all possible combinations of such conditions are consistent with the fusion of the principal fields. For instance, one has

$$\mathcal{Z}_{(1+2|1+2)} = \chi_I + \chi_\varepsilon. \quad (16)$$

The above relation is consistent with the fusion $\Phi^1 \times \Phi^{-1} = I + \varepsilon$, associated to the spin boundary configuration $(1 + 2|1|1 + 2)$ in the limit in which the two points where the boundary conditions change approach each other.

3.3 Spin boundary states in the \mathcal{Z}_4 spin model

The principal primary fields of the \mathcal{Z}_4 theory are shown in Tab.2. In this table, the fields $\Psi^{\pm 1}, \Psi^2$ generate, together with the identity I , the Z_4 parafermionic algebra. Moreover, the fields Ψ^2 , together with ε are the only neutral fields in the \mathcal{Z}_4 theory. In general the number of neutral operators is equal to the dimension of the phase space of the Z_N spin model. It is peculiar of the \mathcal{Z}_N theory with N even, $N = 2n$, that one of these neutral fields coincides with the current Ψ^n .

Analogously to the case of the \mathcal{Z}_3 theory discussed above, one can group the above fields into three representation modules, $\{I, \Psi^1, \Psi^{-1}, \Psi^2\}$, $\{\Phi^{1/2}, \varepsilon', \varepsilon'', \Phi^{-1/2}\}$ and $\{\Phi^1, \varepsilon\}$. Correspondingly, the boundary states will transform under a Z_4 transformation as:

$$\begin{aligned}
|\overline{0, 0}\rangle &\rightarrow |\overline{0, 2}\rangle \rightarrow |\overline{0, 4}\rangle \rightarrow |\overline{0, 6}\rangle \rightarrow |\overline{0, 0}\rangle \\
|\overline{1/2, 1}\rangle &\rightarrow |\overline{1/2, 3}\rangle \rightarrow |\overline{1/2, 5}\rangle \rightarrow |\overline{1/2, -1}\rangle \rightarrow |\overline{1/2, 1}\rangle \\
|\overline{1, 0}\rangle &\rightarrow |\overline{1, 2}\rangle \rightarrow |\overline{1, 0}\rangle.
\end{aligned} \quad (17)$$

Conformal boundary states in the spin representation

In the Z_4 model the spin can take the value 1, 2, 3 or 4. It is natural to consider the boundary spin configurations which generalize the Z_3 spin model. Using the notations of the previous paragraph, we

consider spin boundary configurations which are the natural extension of the one seen in the three-states Potts model:

- *free*: $1 + 2 + 3 + 4$.
- *fixed*: 1, 2, 3 or 4.
- *mixed*: Three types of mixed boundary conditions: a) $1 + 2, 2 + 3, 3 + 4, 1 + 4$, b) $1 + 3, 2 + 4$ and c) $1 + 2 + 3, 2 + 3 + 4, 3 + 4 + 1, 1 + 4 + 2$.

Contrary to the case of the three-states Potts model, the Z_4 transformations of the boundary states, consistent with (17) and (10) are not sufficient to identify all the boundary states. We have thus computed numerically the partitions (9). The numerical implementation is done with a transfer matrix. In order to compute $\mathcal{Z}_{(A|B)} \simeq \chi_\Delta$, it is convenient to work with an infinitely long strip of width L with boundary conditions A and B [23]. The corresponding dominant character χ_Δ is identified by computing the subdominant corrections in :

$$\log(\mathcal{Z}_{(A|B)}) \simeq a_0 + \frac{a_1}{L} + \pi \frac{(c/24 - \Delta)}{L^2} . \quad (18)$$

Here a_0 is associated to the bulk free energy while a_1 is a boundary term corresponding to the fixed boundary conditions A and B . We did the following identifications:

$$\begin{aligned} \mathcal{Z}_{(1|1)} &= \chi_I, & \mathcal{Z}_{(1|2)} &= \chi_{\Psi^1}, & \mathcal{Z}_{(1|4)} &= \chi_{\Psi^{-1}}, & \mathcal{Z}_{(1|3)} &= \chi_{\Psi^2} \\ \mathcal{Z}_{(1|1+2)} = \chi_{\Phi^{1/2}} &= \chi_{\Phi^{-1/2}} = \mathcal{Z}_{(1|1+4)}, & \mathcal{Z}_{(1|2+3)} &= \mathcal{Z}_{(1|3+4)} = \chi_{\epsilon'} = \chi_{\epsilon''} . \end{aligned} \quad (19)$$

The mixed boundary conditions of type a) have been discussed in [26] where the infra-red behaviour of a \mathcal{Z}_N theory with free boundary conditions has been studied. In [26], the RG flow is characterized by a flow from the free boundary conditions to the four stable fixed points associated to the spins taking a fixed value on the boundary. These results generalize the boundary RG flow studied in [25]. With a fine tuning of the boundary perturbation parameters [26], the free b.c. flows to the others four mixed boundary states of type a).

The identifications of the spin boundary states associated to $|\overline{1}, \overline{0}\rangle$ and $|\overline{1}, \overline{1}\rangle$ remain still ambiguous. Indeed our analysis could not discriminate between the possible identifications:

$$\mathcal{Z}_{(1|1+3)} = \chi_{\Phi^1} \quad \mathcal{Z}_{(1|2+4)} = \chi_\epsilon \quad (20)$$

or

$$\mathcal{Z}_{(1|1+2+4)} = \chi_{\Phi^1} \quad \mathcal{Z}_{(1|2+3+4)} = \chi_\epsilon . \quad (21)$$

Below in the paper we will discuss the boundary conditions $(1 + 2|3 + 4)$ which, as we will see, are related to the interface studied in [15]. We have verified numerically that $\mathcal{Z}_{(1+2|3+4)} \simeq \chi_\epsilon$. This is consistent with the identifications (19) and with the operator fusion $\Phi^{1/2}\epsilon' = \epsilon + \dots$, determined by the operator algebra [30]. Note that the identification of the b.c.c. operator transforming in the ϵ representation as the one which generates the condition $(1|2 + 3 + 4)$ has been proposed in [12]. In particular this would support the fact that the b.c.c operator transforming as ϵ is related to such boundary conditions [15].

One last remark: analogously to the Z_3 case, besides the fields shown in Tab. 2, related to the abelian Z_4 sector of the theory, there are a set of fields R related to the Z_2 reflections of the dihedral Z_4 group. We have verified that $\mathcal{Z}_{1,free} = \chi_{R_0}$, where R_0 is the (twist) field with dimension $3/24$ considered in [12].

4 Boundary Interfaces.

We will first present the results obtained by measuring interfaces connecting two points of a lattice in analogy with the chordal SLE interfaces defined in the critical $O(n)$ model. As already discussed in section 2, the Z_4 spin model generalize the fourth-states Potts model. In the Potts model, one can in general consider either geometrical interfaces bounding spin clusters [31], *i.e.* group of spins with the same value, or Fortuin Kastelyn (FK) clusters [34, 35]. In [11], we explained that only geometrical interfaces can be defined for the Z_N spin models since the FK clusters do not percolate at the critical point.

We generated these geometric interfaces by simulating finite square lattices of size $L \times L$ with certain boundary conditions ($A_1 + A_2 \dots | B_1 + B_2 \dots$). This notation means that we set one half of the boundary spins to take the values $A_1 + A_2 + \dots$ and the other half the values $B_1 + B_2 + \dots$. Moreover, we impose that the change from one condition to the other is on the middle of the two opposite borders of the square lattice. Then, for each spin configuration, there is an interface defined as the line on the dual lattice separating the A_i spins connected to one boundary from the B_i spins connected to the other boundary.

The result for the interface associated to the condition $(1|2 + 3 + 4)$ was already presented in [10] where we found a value of the fractal dimension d_f compatible with the value $1 + 10/24$ predicted in [12]. Note that, as we mentioned in the previous section, the scenario proposed in [12] is based on the hypothesis that the b.c.c operator associated to $(1|2 + 3 + 4)$ transforms as in the representation $|1, 0\rangle$ of dimension $1/3$. Naturally, this would be consistent with the identification (21). In order to have a more general picture, we have systematically analyzed boundary interfaces associated to differed boundary conditions, mainly inspired by the classification discussed in the previous section.

Before presenting the main results, we briefly explain how the fractal dimension of these interfaces has been obtained. In order to generate the configurations, we choose the Ising representation (4) for which it is possible to use a cluster algorithm [36] much more efficient than standard Monte Carlo [11]. For each type of boundary conditions, measurements were performed on systems up to the linear size 1280. For each sizes we first determined the autocorrelation time $\tau(L)$ and we average over $N(L) \times \tau(L)$ with $N(L) = 1\,000\,000$ for $L < 160$, $N(160) = 500\,000$, $N(320) = 250\,000$, $N(640) = 100\,000$ and $N(1280) = 50\,000$. A typical value for the autocorrelation time is $\tau(L = 640) \simeq 10000$ for the boundary condition $(1|2)$ and of the same order for other boundary conditions and the same linear size. The fractal dimensions are obtained in the following way. For each linear size L , we determine the average length of the interface $l(L)$ which should scale as

$$l(L) \simeq L^{d_f}. \quad (22)$$

Then we obtain the effective dimension as

$$d_f \left(\frac{L_1 + L_2}{2} \right) = \frac{\log(l(L_1)/l(L_2))}{\log(L_1/L_2)}, \quad (23)$$

where L_1 and L_2 are two different linear sizes of the square lattice.

In Fig. 1a) we present the effective fractal dimensions so computed for the four type of interfaces associated to the $(1|2 + 3 + 4)$, $(1 + 3|2 + 4)$ and $(1 + 2|3 + 4)$ and $(1|2)$ boundary conditions. The conditions $(1 + 2|3 + 4)$

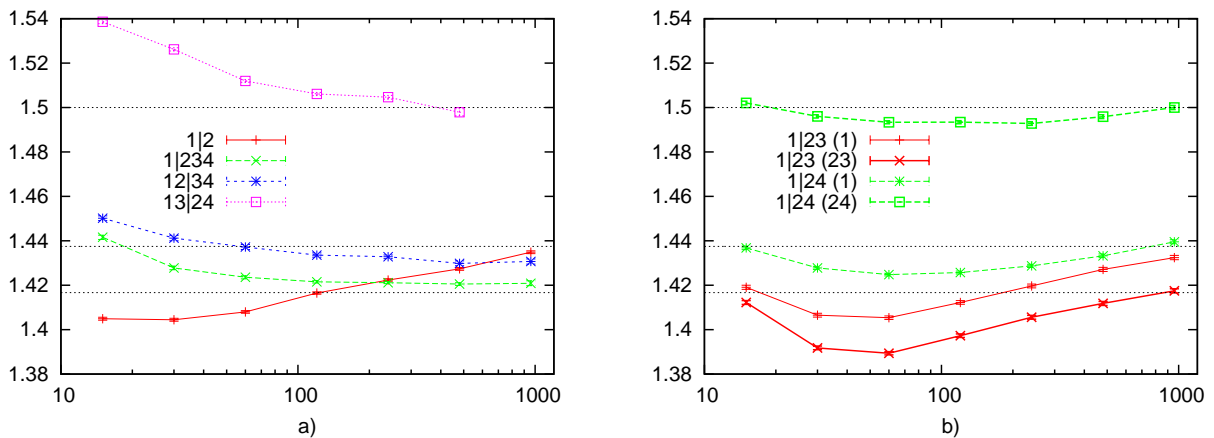


Figure 1: Effective exponents obtained for different interfaces. The three dashed lines correspond to $1 + 10/24$, $1 + 7/16$, $3/2$ as discussed in text.

or $(1 + 3|2 + 4)$ are particularly interesting as they are, besides the condition $(1|234)$, the only other ways for defining a single interface for this model. As one can see from Fig. 1a), we measured a value for the

fractal dimension of the interface $(1+2|3+4)$ which is slightly bigger than the one measured for the $(1|234)$ interface. Even with the large amount of statistics that we have accumulated for this point, it is not possible to decide if the asymptotic value will converge to the same value as for the condition $(1|2+3+4)$ or not. Note that the condition $(1+2|3+4)$ was also considered in the recent work who obtained similar results, namely $d_f = 1.4226(13)$ [15, 37].

On the contrary, for the condition $(1+3|2+4)$ one clearly sees that the value is completely different and seems to converge to the value $d_2 \simeq 3/2$. Few comments are in order. For this condition we do not have data for larger sizes. This is due to the fact that the cluster algorithm is much less efficient for studying this interface. To be more precise, the cluster algorithm is not able to take into account the $(1+3|2+4)$ boundary conditions since the algorithm works for each copy of the Ising model separately [36]. Thus one can only change a spin $S = 1(\sigma = +; \tau = +)$ in either $S = 2(\sigma = +; \tau = -)$ by updating the copy σ or in $S = 4(\sigma = -; \tau = +)$ by updating the copy τ . The direct change $S = 1 \rightarrow S = 3$ can not be done within this algorithm. Since on one border the spins $S = 1$ or 3 , then these spins will be frozen, the same being true for the other part of the border where we impose $S = 2$ or 4 . Thus for this type of boundary conditions, we consider a more complicated algorithm in which we alternate cluster update with standard Monte Carlo updates on the border. Another intriguing observation concerns the obtained value $d_2 \simeq 3/2$. In fact, for this choice of boundary conditions, a fractal dimension compatible with $d_2 \simeq 3/2$ is obtained all along the AT line, [38]. Moreover, in the next section, we show that we find bulk interfaces with fractal dimension d_2 . The fact that we obtain the value d_2 appear to us natural, even if we do not have any strong argument. Indeed it is well known that the value d_2 is the fractal dimension of certain interfaces related to the level lines of the Gaussian free field compactified on a circle [16, 17, 18]. As we have seen in the section 2, the Z_4 spin model on the critical line is also described by a $c = 1$ CFT which is the free Gaussian field compactified on the Z_2 orbifold, $\sqrt{2} \leq r^{orb} \leq 2$. It is thus natural to ask whether these interfaces $(1+3|2+4)$ can be somehow related to an *SLE* process with $\kappa = 4$.

We also report here other cases of boundary conditions. They are $(1|2)$, $(1|3)$, $(1|2+3)$ and $(1|2+4)$. The cases $(1|2)$ and $(1|3)$ generate two interfaces: an interface separates the spins connected to the boundary "1" on one side and spins 2, 3, 4 on the other side while the second interface separates spins 2, 3, 4 with spins connected to the boundary 2 or 3. By symmetry arguments, one can see that each of these two interfaces is equivalent ¹. In Fig. 1a), we show the effective fractal dimension for the case $(1|2)$ and we average over the two interfaces. The result for the case $(1|3)$ is identical except finite size corrections for the smaller sizes, thus we do not show the fractal dimension for this case. The value obtained for the largest sizes is $d_f \simeq 1.435$ which is clearly different from d_1 . We observe that this value, that we will call d_3 , is very close to the value $1 + 7/16$. In [39, 40, 41], it was shown that the interfaces related to an holomorphic operator with spin s are described by *SLE* $_{\kappa^{(s)}}$ with $\kappa^{(s)} = 8/(1+s)$. Here we just notice that the value $1 + 7/16$ corresponds to $1 + \tilde{\kappa}/8$ with $\tilde{\kappa} = 16/\kappa^{(s)}$ and $s = 3/4$ which is the dimension (spin) of the holomorphic current $\Psi^{\pm 1}$. As seen in section 3, the parafermionic current $\Psi^{\pm 1}$ is associated to the $(1|2)$ boundary conditions. This value is also compatible with the value reported for bulk fractal dimension in [11]. We will come back on this point in the next section. The last two cases are a little bit more complicated. For $(1|2+3)$ we have again two interfaces but now these two interfaces do not need to be equivalent. The first interface separates 1 from 234 while the second interface separates 23 from 14. In Fig. 1b), we show the fractal dimension for each interface. It is clear that they are not equal. For both interfaces, we observe strong finite size effects, but the difference between the two fractal dimensions remains near constant as we increase the linear size L . And it seems that the fractal dimension associated with interface bounding the domain connected to the boundary with $S_i = 1$ converges towards d_3 while the fractal dimension of the other interface converges towards d_1 . For the last case $(1|2+4)$ we observe again two fractal dimensions. The one associated to the interface bounding the domain connected to the boundary with $S_i = 1$ converges towards d_3 again, while the second fractal dimension converges towards d_2 .

To summarize the numerical findings, we obtain fractal dimensions which can be grouped in three parts.

¹In [31] similar boundary conditions were considered for the three-states Potts model and called "fixed". In this study, the authors separate the interfaces in a "composite" part and a "split" part and claimed that the fractal dimension associated to the "split" part ($\simeq 1.589$) was much larger than the one expected for spin cluster boundaries and obtained for "fluctuating" boundary conditions $(1+10/24 \simeq 1.41667)$. In fact the difference in these fractal dimensions is due to the existence of strong finite sizes corrections for the "split" part with "fixed" boundary conditions as we have checked for the three-states Potts model and for the Z_4 spin model [38].

A first set of fractal dimensions converge to a value close to $d_1 \simeq 1 + 10/24$ and are associated to either $(1|2+3+4)$ and one of the fractal dimension of $(1|2+3)$. A second set of fractal dimensions converge towards $d_2 \simeq 3/2$ and are associated to $(1+3|2+4)$ and one of the fractal dimension of $(1|2+4)$. The last set of fractal dimensions converge to a value close to $d_3 \simeq 1 + 7/16$ and are associated to the fractal dimension of $(1|2)$ or the second fractal dimension for $(1|2+3)$ and $(1|2+4)$.

Finally the fractal dimension for $(1+2|3+4)$ takes a value between d_1 and d_3 , it is difficult to conclude definitely for this case.

5 Bulk interfaces

In [11] we determined the fractal dimension of interfaces around finite clusters in the bulk. This measurement was done by considering any type of clusters, *i.e.* a geometrical cluster of spins of any fixed value surrounded by spins with a different value. But since we observed in the previous section that the fractal dimension can depend on the type of interface and on particular in the number of allowed values on each side, we will check now if a similar property also occur for finite size clusters. The goal is to check if the fractal dimension can depend on the number of allowed values of the geometrical clusters and how. In our simulations, we considered a square lattice with periodic boundary conditions. For a given geometrical cluster we computed the average area A defined as the number of spins inside a contour of length l . These two quantities are related to the fractal dimension in the following way :

$$A(l) = l^\delta \quad (24)$$

with $\delta = 2/d_f$. To obtain this last relation, one note that $A(l) = R^2$ with R the radius of gyration which is related to the length of the contour by $l = R^{d_f}$.

We can then perform a direct measurement of the distribution of the clusters in function of their length recording for each length the average area. In order to compare the different type of clusters, we first use the global Z_4 symmetry for each configuration. We rotate the spins such that the majority of them take the value "1". Next we compute all the type of spin clusters. The simplest case is the clusters "1" which corresponds to spins of value "1" surrounded by spins taking another value. We can then define the associated distribution $D_1(A, l)$ which counts the number of such clusters with area A and length of the surrounding interface l . One can define three one-spin distributions, D_1, D_2, D_3 (by symmetry, the distribution D_4 is equivalent to D_2). Next we have to consider two-spins distributions corresponding to clusters of spins taking two fixed values surrounded by spins taking the remaining values. We have to consider $D_{12}, D_{13}, D_{23}, D_{24}$ and similarly for the three-spins, we have to consider $D_{123}, D_{124}, D_{234}$. For each of these distributions, one can then extract a fractal dimension by using eq.(24). Finally in order to get a precise measurement of δ , we compute the integrated quantity corresponding to

$$X(l_{max}) = \int^{l_{max}} A(l) \simeq l_{max}^{1+\delta} . \quad (25)$$

The values of $d_f = 1/\delta$ is obtained from the ratio $X(l_{max})/X(l_{max}/2)$ for increasing l_{max} for the different types of clusters.

A first result is that the fractal dimension is the same for any type of cluster with equal sign even if we have introduce an explicit breaking of symmetry by imposing the majority rule. We will only consider the case of D_2 in the following. The same result is also obtained for the clusters with spins restricted to three values for which we will only consider the case of D_{234} . For the clusters with spins restricted to two values, we observe two behaviors, one for D_{12} with the same result as for D_{23} and a second one for D_{13} with the same result as for D_{24} .

In Fig. 2, we present the obtained fractal dimensions versus l_{max} . This figure contains many similarities with Fig. 1a). Again we obtain a fractal dimension 1.5 associated with clusters containing spins of value 1, 3 or 2, 4. This fractal dimension is in very good agreement from the one obtained for the interface $(1+3|2+4)$. The second fractal dimension is associated to clusters with one value ((2)) and seems to be in correspondence with the interface $(1|2)$. It is also natural to associate the fractal dimension for clusters with three values ((2+3+4)) with the one from the interface $(1|2+3+4)$. The last one $(1+2)$ or $(3+4)$ is then associated

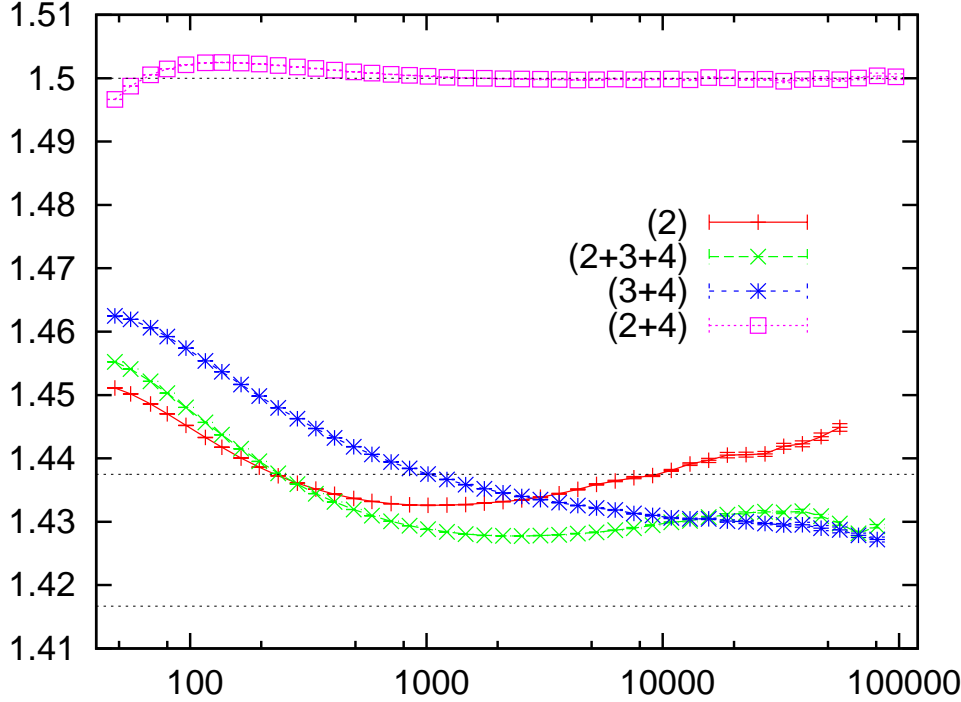


Figure 2: Effective exponents in the bulk obtained from eq.(25) for Z_4 .

to the fractal dimension of the interface $(1 + 2|3 + 4)$. The interesting observation is that, in the bulk, the fractal dimensions for the clusters with three values seem to coincide with the one for $(1 + 2)$ in the large size limit. This would then confirm that the two fractal dimensions for the interfaces $(1|2 + 3 + 4)$ and $(1 + 2|3 + 4)$ would coincide in the large size limit.

An important observation is that the fractal dimension $d_2 \simeq 3/2$ is associated to objects arising naturally in the high temperature expansion of the AT Model [2, 21, 42]. Indeed, by replacing in (4) (σ_i, τ_i) by $(\sigma_i, t_i = \sigma_i \tau_i)$ then clusters of either $t_i = +1$ or $t_i = -1$ are natural objects to consider. Indeed, as shown in [2, 21, 42], after performing an Ising high-temperature expansion, the partition function defined with the Hamiltonian (4) represses as

$$Z_{H_{AT}} \simeq \sum_{\text{graphs}} (\tanh 2K)^{l+d}, \quad (26)$$

with the sum running on two types of (non intersecting) graphs : polygons \mathcal{L} on the lattice coming from the expansion of σ_i and polygons \mathcal{D} on the dual lattice coming from the low-temperature expansion of t_i and the total numbers of bonds on each lattice is l and d respectively. The boundary of the clusters forming \mathcal{D} corresponds to the bulk interface with the fractal dimension d_2 .

6 Summary and conclusions

In this paper we have considered the Z_4 spin lattice model at the FZ critical point. The FZ point is described in the continuum limit by the parafermionic Z_4 CFT which is a rational CFT with extended Z_4 symmetry. Contrary to the case of the CFTs based on Virasoro algebra, the behavior of geometric objects for general extended RCFTs is far to be understood. In order to provide new insights into this problem, we have considered different types of boundary and bulk spin cluster interfaces which can be naturally defined in the Z_4 spin lattice model. In particular, we have computed their fractal dimensions at the FZ point. The basic

idea behind the analysis presented here and in previous works [10, 11, 12] is that, analogously to the critical $O(n)$ models described by Virasoro CFT's, the geometrical properties of a Z_4 spin lattice model at the FZ point should be related to the classification and properties of the primary operators of the corresponding extended algebra, in this case the parafermionic algebra.

First we considered the lattice model on a bounded domain. We studied interfaces which origin and terminate at boundary points and which are generated by imposing certain boundary spin configurations. We examined all kind of boundary spin configurations whose definition is naturally suggested by the Z_4 spin symmetry of the model. Despite the great number of interfaces we considered, the numerical results indicate that there are only three values of fractal dimension, d_1, d_2 and d_3 , characterizing the critical behavior of these boundary interfaces. We showed that this result can be somehow understood on the basis on the classification of conformal invariant boundary states. For this purpose, we have discussed the identification of conformally boundary states, as predicted by the boundary RCFT, in terms of boundary spin configurations. We provided evidences that the existence of this three different values can be related to the different representation modules of the parafermionic algebra. For instance, the value $d_1 \simeq 1 + 10/24$, already measured in [10, 11], is associated to the b.c.c. operator of dimension $1/3$ and compatible with the value predicted in [12]. Other interfaces, like the one studied in [15], which seem to have the same fractal dimension d_1 , are associated to conformally boundary conditions which in turn are connected by fusion to this operator. This was in general checked on the basis of our identification of conformal spin boundary states and fusion rules of the correspondent Z_4 primaries. For the values d_2 and d_3 there are no theoretical arguments to derive them. However we stressed that i) the value d_2 obtained is very close to the fractal dimension $3/2$ of SLE interfaces defined as level lines of free Gaussian fields and related to a b.c.c. operator of dimension $1/4$ [16, 17, 18]. This is particularly interesting as the Z_4 is also a $c = 1$ theory which can be described by a free Gaussian field compactified on a orbifold; ii) the value $d_3 \sim 1 + (1 + s)/4$ where $s = 3/4$ is the dimension of the Z_4 holomorphic current. It is natural to ask whether there is some connection to the $SLE_{8/(1+s)}$ interfaces which are related to an holomorphic operator with spin s [39, 40, 41].

We have further investigated different interfaces which has been opportunely defined in the bulk. The results obtained for the bulk interfaces confirmed the scenario emerging from the study of boundary interfaces. Indeed, we could observe there are indeed three different values of fractal dimension which are compatible with the values d_1, d_2 and d_3 . Interestingly the interfaces having the fractal dimension d_2 correspond to the spin cluster boundaries which appear in the high-temperature expansion of the AT model [2, 21, 42].

We conclude by emphasising that our results on critical interfaces at the parafermionic point of the AT are expected to unveil general aspects of geometrical objects of critical AT model, and thus of $c = 1$ critical theories [38]. Therefore, as a theoretical understanding is still lacking, we believe that the results presented here can represent good motivation for studying critical interfaces in free Gaussian field on an orbifold.

References

- [1] see for instance B. Duplantier, Les Houches 2005 Lecture Notes, Session LXXXIII, 101, Elsevier (2006), math-ph/0608053.
- [2] B. Nienhuis, in *Phase Transitions and Critical Phenomena*, edited by C. Domb and J. L. Lebowitz (Academic, London, 1987), Vol. 11, p.1.
- [3] H. Saleur and B. Duplantier, Phys. Rev. Lett. **58**, 2325 (1987).
- [4] W. Janke and A. M. J. Schakel, Braz. J. Phys. **36**, 708 (2006).
- [5] see for instance J. Cardy, Annals Phys. **318**, 81-118 (2006) or I.A. Gruzberg, J. Phys. **A39**, 12601-12656 (2006) and references therein.
- [6] P. Di Francesco, P. Mathieu and D. Sénéchal, *Conformal Field Theory*, Springer, New York, 1997.
- [7] M. Bauer and D. Bernard, Ann. Henri Poincaré **5**, 289 (2004).
- [8] I. Affleck and F. D. M. Haldane, Phys. Rev. B. **36**, 5291 (1987).
- [9] V. A. Fateev and A. B. Zamolodchikov, Phys. Lett. **92A**, 37 (1982).
- [10] M. Picco and R. Santachiara, Phys. Rev. Lett. **100**, 015704 (2008).
- [11] M. Picco, R. Santachiara and A. Sicilia, J. Stat. Mech. (2009) P04013.
- [12] R. Santachiara, Nucl. Phys. **B793**, 396 (2008).
- [13] J. Rasmussen, arXiv:hep-th/0409026.
- [14] E. Bettelheim, I. A. Gruzberg, A. W. W. Ludwig and P. Wiegmann, Phys. Rev. Lett. **95**, 251601 (2005).
- [15] M. Caselle, S. Lottini and M. A. Rajabpour, arXiv:0907.5094.
- [16] O. Schramm and S. Sheffield, Acta Math. **202**, 21 (2009).
- [17] J. L. Cardy, arXiv:math-ph/0412033.
- [18] C. Hagendorf, D. Bernard and M. Bauer, arXiv:1001.4501.
- [19] J. Ashkin and E. Teller, Phys. Rev. **64**, 178 (1943).
- [20] R. J. Baxter, *Exactly Solved Models in Statistical Mechanics*, Associated Press, London, 1982.
- [21] B. Nienhuis, J. Stat. Phys. **34**, 731 (1984).
- [22] P. Ginsparg, Nucl. Phys. **B 295**, 153 (1988).
- [23] J. L. Cardy, Nucl. Phys. **B 324**, 581 (1989).
- [24] H. Saleur and M. Bauer, Nucl. Phys. **B 320**, 591 (1989).
- [25] I. Affleck, M. Oshikawa H. Saleur, J. Phys. A. **31**, 5827 (1998).
- [26] S. L. Lukyanov, Nucl. Phys. **B 784**, 151 (2007).
- [27] C. Mercat and P. A. Pearce, J. Phys. A **34**, 5751 (2001).
- [28] N. Ishibashi, Mod. Phys. Lett. **A 4**, 251 (1989).
- [29] J. L. Cardy, Nucl. Phys. B **240**, 514 (1984).
- [30] J. Maldacena, G. Moore and N. Seiberg, JHEP 0107:046 (2001).

- [31] A. Gamsa and J. L. Cardy, J. Stat. Mech. (2007) P08020.
- [32] V. A. Fateev and A. B. Zamolodchikov, Sov. Phys. JETP **63**, 913 (1986).
- [33] J. Fuchs and C. Schweigert, Phys. Lett. **B 441**, 141 (1998).
- [34] F. Gliozzi and M. A. Rajabpour, arXiv:1003.3147.
- [35] D. A. Adams, L. M. Sander and R M. Ziff, J. Stat. Mech. (2010) P03004.
- [36] S. Wiseman and E. Domany, Phys. Rev. **E 48**, 4080 (1993).
- [37] M. A. Rajabpour, private communication.
- [38] M. Picco and R. Santachiara, in preparation.
- [39] V. Riva and J. L. Cardy, J. Stat. Mech. (2006) P12001.
- [40] M. A. Rajabpour and J. L. Cardy, J. Phys. A. **40**, 14703 (2007).
- [41] Y. Ikhlef and J. L. Cardy, J. Phys. A. **42**, 102001 (2009).
- [42] H. Saleur, J. Phys. A **20**, L1127 (1987).